A. COVER PAGE FINAL TECHNICAL REPORT - AWARD G11AP20008

1. Project Title: **Fault Gouge Rheology During Earthquake Slip: Experimental Investigation**

2. Principal Investigator(s):

Dr. Ze'ev Reches
School of Geology and Geophysics
U of Oklahoma
100 E Boyd St.
Norman, OK 73019
Tel. 405-321-3157, Fax. 405-325-3140
email: reches@ou.edu

3. Proposed Start Date: December 1, 2010

4. Proposed Duration: 12 months

B. TABLE OF CONTENTS

A. Cover Page Final Technical Report - Award No. G11AP20008 1
B. Table of contents 1
C. Abstract 2
Fault Gouge Rheology During Earthquake Slip: Experimental Investigation 2
D. Background: Dynamic weakening by gouge and powders 2
E. Present investigation 4
Main objectives 4
Building a Confine ROtary Cell, CROC 4
The control software 5
Preliminary results 10
Planned experiments 13
E. References 14

C. ABSTRACT

FAULT GOUGE RHEOLOGY DURING EARTHQUAKE SLIP: EXPERIMENTAL INVESTIGATION

We present here a final report of the 12 months project. This period was devoted primarily to development of experimental capabilities to test fault gouge under controlled conditions. Current status of these developments and the on-going and future experimental work are reported.

Existing experimental system. The rotary shear system in the University of Oklahoma allows for experimental analysis of rock friction under the mechanical conditions of a fault-zone during dynamic rupture. The system can simultaneously apply large displacements of tens of meters, slip velocity of 0.001-2.0 m/s, normal stress of 35 MPa, and slip rise time of a fraction of a second. The system monitors (up to 10 kHz) the slip velocity, shear and normal loads, dilation across the slipping surfaces, and the temperature within the sample. Experimental results on dry, solid rock samples were presented in the original proposal.

Proposed research in NEHRP2011. We proposed to develop the next stage in earthquake simulation by building a Confined Rotary Cell (CROC) as a complementary component to ROGA, and to use CROC for testing confined gouge. The proposal included two main parts: testing the frictional behavior of confined, dry gouge, and building the CORC for elevated pore-pressure.

Accomplishments. We completed the following components: 1. Building the CROC assemblage as proposed; 2. Improving CROC original design so it is suitable for both dry powder as well as pore-pressure controlled experiments; 3. Running successful dry-powder tests with CROC including its calibration; 4. Design and programming of a new operating software (LabView) with flexible control of slip velocity, shear power density, and pore-pressure; 5. Purchasing and testing a syringe pumps system for pore-pressure/permeability measurements (not tested yet in CROC).

On-going and near future work. We currently work on: 1. Improving the calibration of CROC; 2. Using the current setting of CROC to test dry and wet gouge powders of kaolinite, montmorillonite, quartz, milled granite, and milled gabbro. In the near future, we will switch CROC to its pore-pressure version. This switching is relatively simple (below), and we will test its success on porous quartz powder. We anticipate that the newly acquired experimental techniques will contribute to key questions of earthquake physics as outlined in the original proposal.

This report focuses on our technological accomplishments during the current research period that open the door for promising experimental work on earthquake physics. We do not discuss here the implications of the preliminary results; extensive discussions on the background and approach were presented in the original proposal.

D. BACKGROUND: DYNAMIC WEAKENING BY GOUGE AND POWDERS

Fine-grain powder in fault-zones

Slip along faults in the upper crust is always associated with rock comminution and the formation of non-cohesive gouge powder (Sammis et al., 1986; Wilson et al., 2004; Scholz, 2002). The cohesive fine-grained rocks such as cataclasites and ultracataclasites are also common in fault-zones (Chester & Chester, 2006); they are the lithified variety of the non-cohesive gouge powder. Typically, the fine-grained powders (grain-size < 1 micron) occur in the 1-10 cm thick inner-core of the fault-zone (Chester et al., 1993). It has been suggested that most of the fault slip is localized within this narrow inner-core (e.g., Sibson, 2003; Chester et al., 1993). Laboratory shear experiments reveal similar behavior with grain-size reduction and the formation of fine-grain gouge powder between sliding blocks (Yund et al., 1990; Tullis, 2007). This ubiquitous occurrence of gouge powder in all fault-zones and its apparent associated with their slip implies that gouge powder mechanical behavior may play a significant role in the fault-zone weakening (e.g., Marone, 2004). The potential for gouge weakening is discussed below in light of lubrication models.

Lubrication by fluids and powders

A common lubrication experiment is conducted by shearing oil between a rotating disk that is pressed against a stationary solid disk; the loads, gap between the disks and velocity are controlled or monitored (e.g. Luengo et al., 1996; Lu et al., 2007). The resistance to shear is presented on a diagram, frequently called the Striebeck diagram, that displays "friction" as a function of a dimensionless velocity parameter which incorporates experimental parameters of angular velocity, fluid density, gap dimensions, fluid viscosity, and others (Fig. 1) (Luengo et al., 1996; Brodsky and Kanamori, 2001; Lu et al., 2007). The usage of the dimensionless velocity parameter demonstrates similar behavior for different fluids and conditions. The Striebeck diagram displays hydrodynamic transitions (after Luengo et al., 1996):

(1) At low velocity (=slow strain rate), which is marked as "boundary" regime in Fig. 1, the measured gap between the rotating disks is small and the friction is high. It was suggested that in this regime the asperities of the solids surfaces are in direct contact (the gap is small), and the high friction reflects solid-solid friction (Luengo et al., 1996; Lu et al., 2007);

(2) Under intermediate velocity, marked as "mixed" regime in Fig. 1, the measured gap between the solids increases and the friction drops by 50% to 90%. In this regime, the lubricant penetrates between the two blocks (the gap increases), and reduces the solid-solid contact at the asperities;

(3) Under high velocity, marked "bulk" regime in Fig. 1, the gap further increases and the resistance to slip increases quasi-linearly with velocity. This mode indicates that the asperities are no longer in direct contact (large gap), and the resistance to slip is due to viscous flow in the lubricant (Luengo et al., 1996; Lu et al., 2007).

Dry particulate materials are also used as lubricants in the industry (Wornyoh et al., 2007), and they may be divided into two main types:

(1) **Powder lubricants** are dry, cohesive, soft, fine-grain (< 1 μm) particles that deform under load, and "flow". It was suggested that they adhere to the sliding surfaces, and form a "third body" (Fig. 2) that actually separates the sliding surfaces. The friction resistance is due to shearing of the powder layer (=third body). Macroscopically, the flow of these powders resemble the flow of oil-like lubricants (Wornyoh et al., 2007; Higgs et al., 1999), albeit the flow micro-mechanisms are different

(2) **Granular lubricants** are dry, cohesionless, strong, medium (> 100 μm) to coarse particles. These particles retain their shape under load, and "flow" by sliding and rolling at low velocities, and by inter-particle collisions at high velocities (GRD midi, 2004).

Both types of particulate materials can serve as lubricants as they reduce the friction between the sliding bodies. Particulate materials, primarily nano-powders, were applied to systems operating under extreme conditions of elevated temperature and high pressure, e.g., oil-free, high-load bearing operating at 815°C (Kaur and Heshmat, 2002) or parts of gas turbine engines (Leshchinsky et al., 2002). An outstanding experimental example of dry powder lubrication was presented by Klausner et al. (2000) who sheared dry silica powder and polymer powder in a sealed, rotary cell under shear rates up to ~$3\cdot10^3$ s^{-1}, large displacements (meters), and low normal stress (< 16 kPa). Their experiments display three stages of the apparent friction, μ: (1) μ increases with shear-rate increase at low shear rate (> 600 s^{-1}); (2) large drop in μ as shear-rate further increases to ~1200 s^{-1}; and (3) increase of μ with increasing shear-rate.

Particulate lubrication was considered as a mechanism for earthquake weakening. Mair and Marone (1999) used direct shear experiment with layers of granular materials under σ_n = 25 to70 MPa, relatively low slip velocity of V= 0.001 to 10 mm/s, and cumulative slip up to 20 mm. Based on dilation measurements, they suggested that grain rolling could operate at high velocity and could serve as a frictional weakening mechanism. It was further shown that the shape, dimensions, sorting and rolling configuration (2D versus 3D), have profound effect on the friction magnitude. Brodsky and Kanamori (2001) suggested that gouge flow could reduce the macroscopic frictional resistance during earthquakes by penetration of pressurized fluid-like gouge between contacting asperities. These authors suggested an analogy between gouge behavior and oil lubrication that is described by elastohydrodynamic lubrication (Fig. 1) (Luengo et al, 1996).

Possible significance of gouge lubrication

We think that gouge powder (dry or wet) has the potential to control the rate-dependent weakening of major fault-zones. Powders display rich rate-dependent friction modes, and fine-grained gouge (with or without brine) is present in all active fault-zones in the upper crust. The complex rheological properties displayed by fine-grain powders may hold a key to the understanding of earthquake dynamic instability.

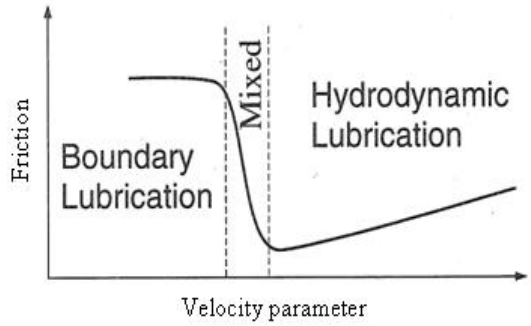

Fig. 1. A schematic presentation of the resistance to shear (=friction) as function of a velocity parameter during lubrication. At low velocity (left), the friction is high due to direct solid-solid contacts. At the mixed regime (center), the friction drops as the lubricant partly separates the two blocks and asperity contacts are reduced. In the hydrodynamic regime (right), the friction increases with velocity due to flow resistance in the lubricant.

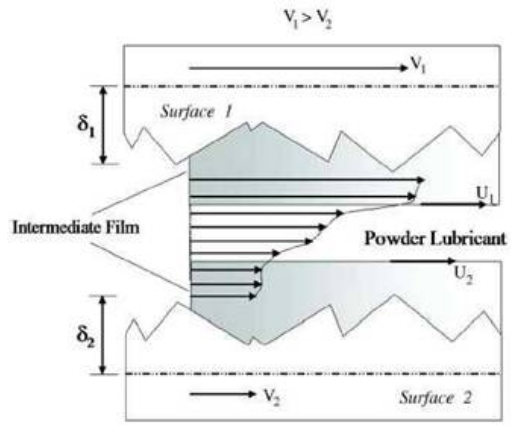

Fig. 2. A model of dry powder lubrication; part of the powder adheres to the sliding surfaces, and the central part of the powder behaves form a "third body" that behaves as a pseudo-hydrodynamic lubricant (from Wornyoh et al., 2007).

E. PRESENT INVESTIGATION

MAIN OBJECTIVES

We experimentally study the mechanical properties of fault gouge under in-situ earthquake conditions. Main objectives in the present project were (1) to build a Confine ROtary Cell (CROC) system, (2) to program a flexible control software, and (3) to conduct preliminary experiments. The existing apparatus, ROGA (Rotary Gouge Apparatus), was described in the original proposal and we described below the results of the current accomplishments.

BUILDING A CONFINE ROTARY CELL, CROC

Dry-powder option

Major effort was devoted to design and building the confined cell, CROC. The construction was done by Entek Corporation, Norman, OK. CROC includes (Figs. 3, 4) a ring-shape gouge chamber of 62.5 mm inner diameter, 81.25 mm outer diameter, and up to 3 mm thick gouge sample. The ring-shape geometry reduces the velocity difference between inner and outer diameters to ~ 15%. The lower, rotating part of CROC contains the sample chamber (left side in Fig. 4). The upper, stationary part (right side in Fig. 4) includes the loading hollow cylinder (grooved surface), and the connections for temperature and dilation measurements, and pore-pressure control.

The critical component of CROC is the sealing assembly. Each side of the gouge chamber has two pairs of industrial, high performance lip seals. We use spring-energized, self-lubricating, teflon-graphite seals manufactured by T-Lon (t-lon.com). These seals are built for pressures up to 280 MPa, temperature up to 250°C for particle media. The space between each of the two sets of seals is pressurized by nitrogen up to the normal stress level. This design generate 'zero-differential pressure' on the inner seal (which is in contact with the gouge powder), and thus it prevents gouge leaks. The nitrogen pressure is continuously

monitored during the tests. The preliminary testing show that the sealing system works as expected with no gouge leaks beyond the pressurized lip (Fig. 5).

Two types of surfaces are in contact with the gouge powder: gently grooved loading surfaces (Fig. 4) or coated with a single later of medium size (250 μm) quartz sand. The quartz sand is glued to the metal surface for good contact with the loose gouge (Fig. 6). The quartz sand coating proved effective in transferring the shear into the powder layer, and reducing (and maybe eliminating) the concentration of shear between the loading metal surface and the powder. This success is demonstrated in Fig. 6 that shows the surface of the loading, upper cylinder with kaolinite powder well attached to the quartz-coated surface. In the future, we will study the dynamic gouge formation, and then the loading surfaces will be made of fine grain rock rings glued to the surfaces.

The assembled CROC can be easily mounted in the loading frame of ROGA (Fig. 7). The stationary top is loaded by the axial hydraulic piston to the selected normal stress. The shear stress in the gouge chamber is measured by the torque monitoring system of the existing ROGA. The upper part also houses the existing systems for dilation measurement of the gouge (Eddy current sensors, Fig. 7), and a thermocouple mounted 1 mm from the sliding surfaces.

Pore-pressure option

The CROC described above is already designed for experiments with pore-pressure. It has two channels that reach the sliding surface in the upper part that can be connected to external fluid pressure pumps through an inlet (Fig. 7). Currently, these channels are blocked by removable metal plugs that can be replaced by plugs made of porous frit (porous ceramic) or open-cell metal foams. These porous plugs will allow inlet of the pore fluid into the powder chamber, and allow pressurization of the powder pore fluid. At the same time, the plugs will block powder leakage.

The pore-pressure will be controlled with a system of two dedicated syringe pumps. We purchased a dual pump 100DX made by Isco-Teledyne (Fig. 8). This system is capable of flow rates from 0.00001-50 ml/minute at pressures to 69 MPa, with a flow accuracy of +/- 0.3%. This system will also be used to measure the gouge permeability before and after the test. With additional small modification of the lower part, we will be able to measure the permeability both parallel and normal to the gouge layer. The critical significance of fault-zone permeability to earthquake and faulting processes has been discussed (Lockner et al., 2000; Noda & Shimamoto, 2005.). The modified CROC will allow to experimentally test these models. The pore-pressure control is already incorporated in our LabView operation software (below). We will start experimentation with pore pressure by May, 2012.

THE CONTROL SOFTWARE

We designed and programmed a new control program in LabView; the front panel of the program, ROGA1.0, is shown in Fig. 9. The program has the following capabilities:

1. High-frequency (5 kHz) control of the following modes of sample shear:
    a. Velocity control, including complex velocity histories (stepping, ramps etc.). This is the common mode in all rotary apparatuses and used by Reches & Lockner (2010).
    b. Power control. Under this mode, the power density, P, on the sample is continuously calculated as $P = \tau \cdot V$, where τ is the shear stress on the sliding sample and V is the slip velocity. The shear stress τ is determined by the rock sample property, and the program adjusts the motor velocity to meet the power history requested by the operator. We think that this mode best fits fault loading during an earthquake.
2. Control file preparation according to operator requests.
3. Monitoring all sensors and saving the data.
4. Inspection and comparison of experimental results.
5. Modification of motor parameters.
6. Control of the syringe pump system for experiments under pore-pressure.

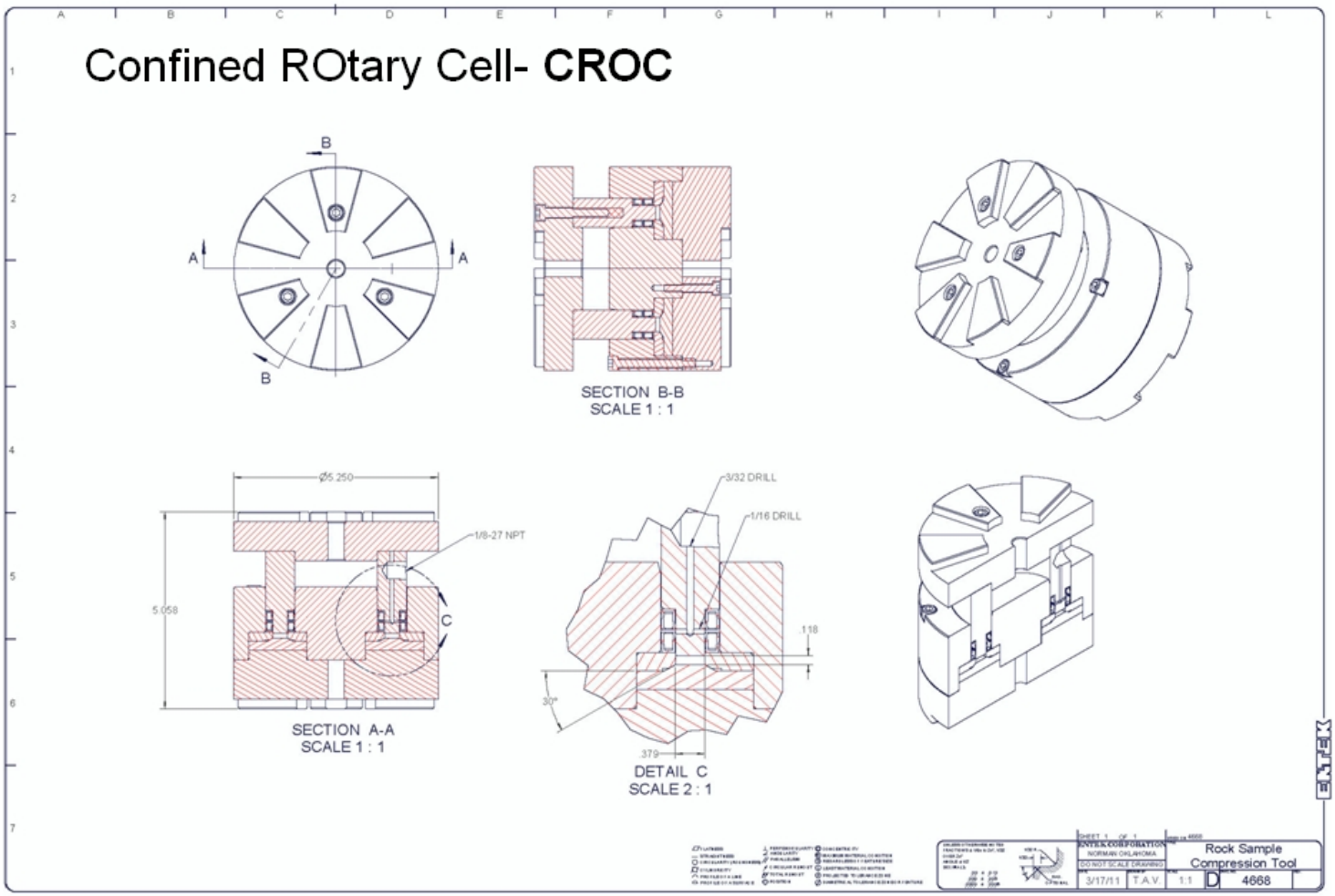

Fig. 3. Production design of CROC, Entek Corporation.

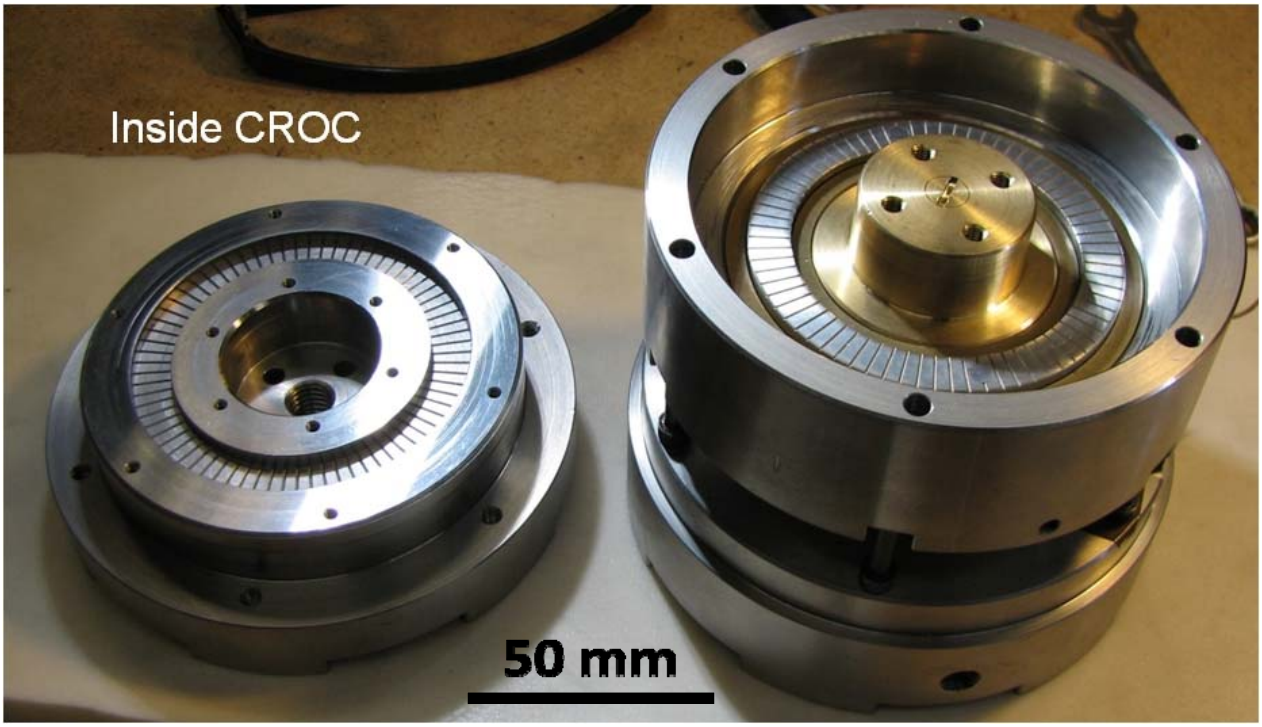

Fig. 4. View inside CROC. Left- Lower, rotating part; grooved ring is the base of the powder chamber. Right- upper stationary part; grooved ring is the surface of the loading hollow cylinder of the normal stress; two tan color rings around the grooved surface are the lip seals; the brass centralizer (see also Fig. 5) is screwed to the lower part.

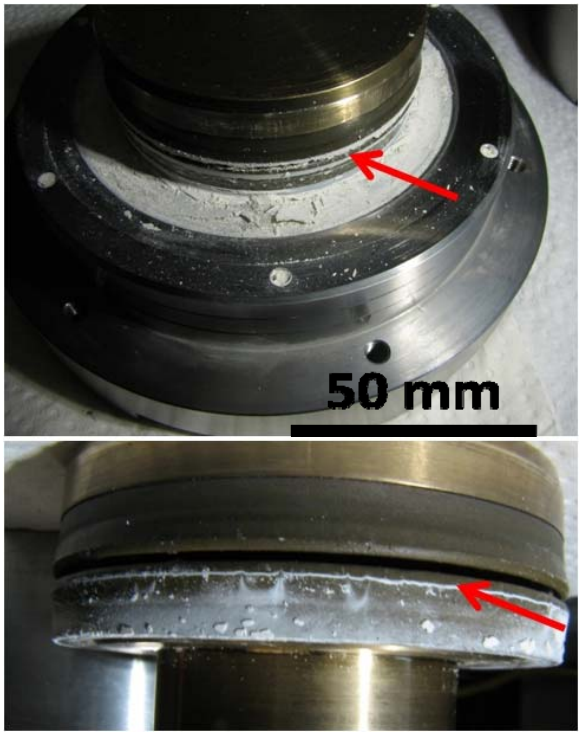

Fig. 5. The lower part after a kaolinite shear experiment. Top. The white ring is the top of the kaolinite layer; note the two tan seals on the brass centralizer; only the lower seal, which was in contact with the powder, is covered with kaolinite to the level of the lip (red arrow). Bottom. Close-up view of the top showing that powder did not pass the lip. Note the space between the two seals which is nitrogen pressurized during the run.

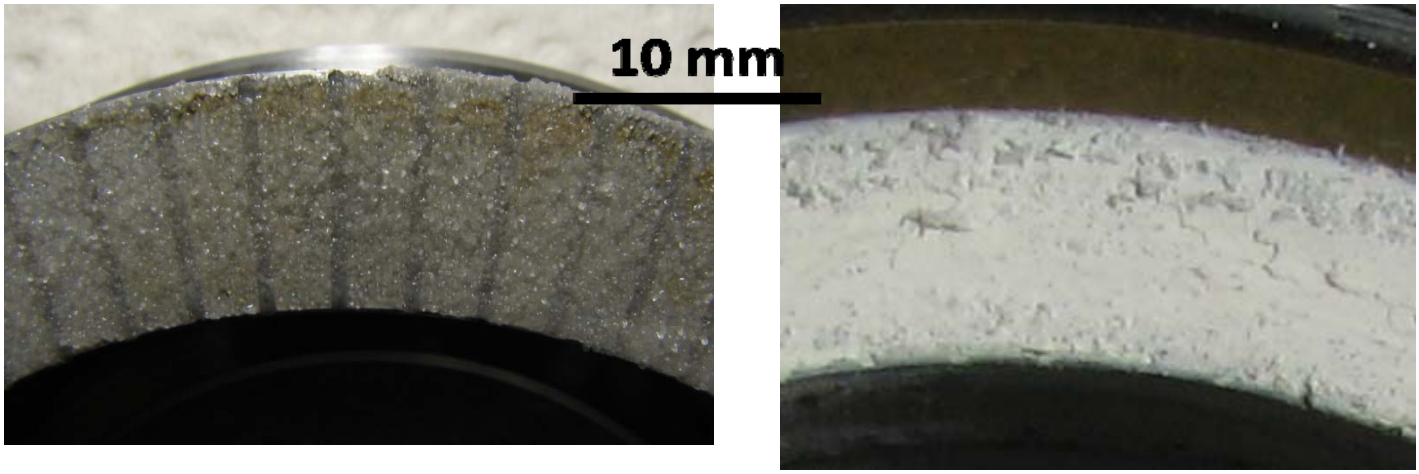

Fig. 6. Partial view of the sand-coated top of the loading hollow cylinder that applies the normal stress (Fig. 4). Left- view before an experiment. Right- view after an experiment; note complete coverage with kaolinite powder indicating that shear occurred within the powder layer (see details in Fig. 13).

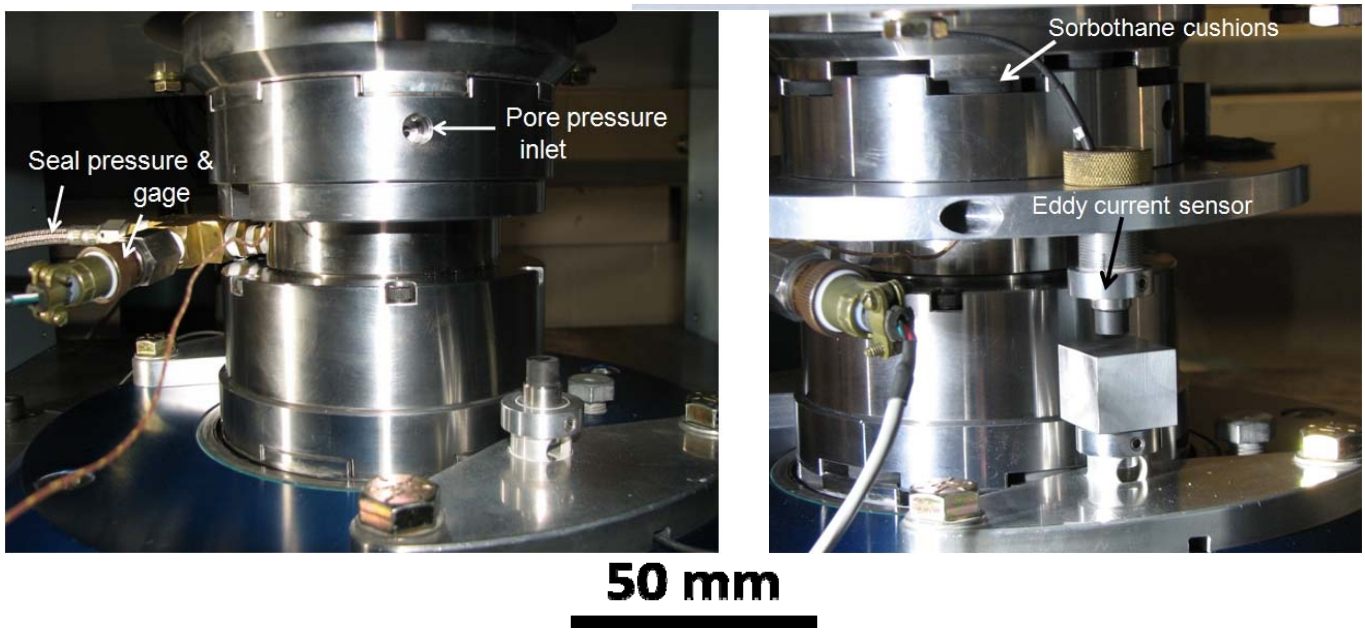

Fig. 7. CROC assemblage mounted in running position in ROGA.

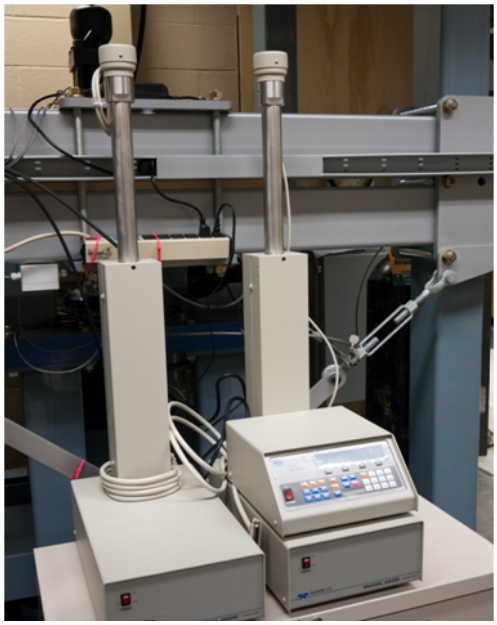

Fig. 8. The dual syringe pumps, 100DX by Isco-Teledyne, next to ROGA apparatus.

Controlling program (LabView)

Fig. 9. The front panel of Roga1.0, the new LabView operation system is post experiment viewing option. Note the multiple tabs at the base that provide versatile control options.

PRELIMINARY RESULTS

Seal calibration

The contribution of the seal system of CROC to the measured torque and normal stress was determined by running it without powder. The empty CROC assemblage was mounted in the loading system (Fig. 7), the seals were pressurized to 500 psi nitrogen, and tests were run at zero axial load at slip velocities up to 0.35 m/s. The results of a typical run (Fig. 10) indicate the following:

1. A normal stress rise of $\Delta\sigma_n < 0.1$ MPa, most likely due to partial leak of pressurized nitrogen into the sample chamber.
2. The torque sensor force (Ts in lbs) varies linearly with slip velocity (V in m/s), as $Ts = 42.7 + 51.3 \cdot V$, and standard deviation is 3.8 lbs. These relations were used to correct stress data in the powder experiments described below.
3. The torque sensor force varies cyclically, probably due to seal pressing during CROC wobbling. One of our near-future objectives is to reduce this artifact.

Preliminary experiments

We used CROC to run a series of 13 experiments with ~2.0 mm thick layer of kaolinite powder to examine CROC operation. The parametric relations of four consecutive experiments, #2010-2013 are presented in Fig. 11 with more details in Fig. 12 for run 2013. This series started with a fresh kaolinite layer, prepared at room-conditions, that was emplaced in the lower part and hand-pressure compacted before run 2010. The upper, loading hollow cylinder was coated with quartz grains (Fig. 6, left). This was a slide-hold series with stepping velocities up to 0.1 m/s (green in Fig. 11), and hold periods of 5 to 9 minutes between the runs. The normal stress was 1.05 MPa, and the cumulative slip distance was 6 m (Fig. 11). The above calibrated relations for seal friction were used to correct the torque and normal stress readings.

The main mechanical observations in these experiments are:

1. During slip, the sample was compacted (negative dilation in Fig. 11) at asymptotically reducing rate. The cumulative compaction was 0.73 mm that accounts for about 1/3 of the initial thickness.
2. Slip initiation after each hold period displays a brief, fast compaction that was followed by a temporal dilation event of 10-30 μm (orange circles in Fig.11, and details in Fig. 12).
3. The sample showed minor, if any, peak frictional strength upon the initiation of runs 2010 through 2012. Run 2013 started with a peak of $\mu \sim 0.9$ (Fig. 12).
4. Experiments 2010-2011 show a steady-state friction of $\mu = 0.24 \pm 0.08$. This value is similar to the steady-state value determined by Brantut et al., (2008).
5. The experiments display general frictional strength increase with cumulative slip and compaction, and did not show a clear strength dependence on slip velocity (Fig. 12).
6. The kaolinite shear led to modest temperature increase of ~12ºC in run 2013 (Fig. 12).

The kaolinite layer was examined after run 2013 with no further microscopic analysis. The main observed features are:

1. Shear accommodation was <u>within</u> the kaolinite layer, and it was not localized at the metal-powder contact (Fig. 13). This featue was achieved thanks to the glued layer of quartz sand on the loading surface (Fig. 6).
2. The sheared layered displayed multiple internal slip surfaces at Riedel shear orientation. These surfaces have slickenside striations with trend parallel to the rotation direction (Fig. 14).

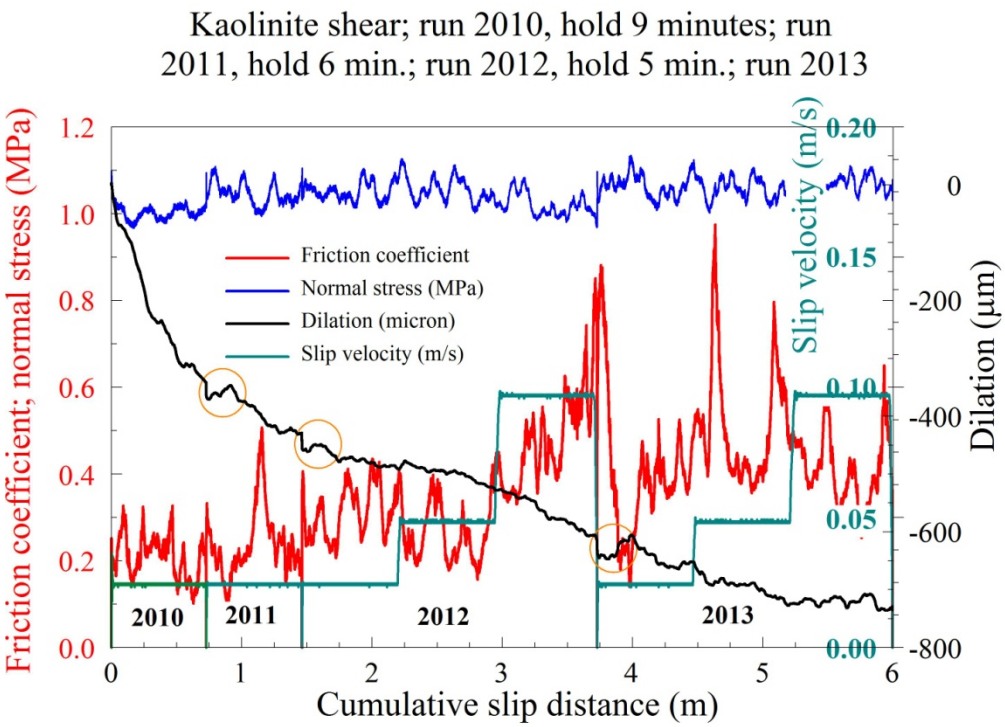

Fig. 11. Parametric observations during a series of slide-hold experiments 2010-2013; see text for discussion.

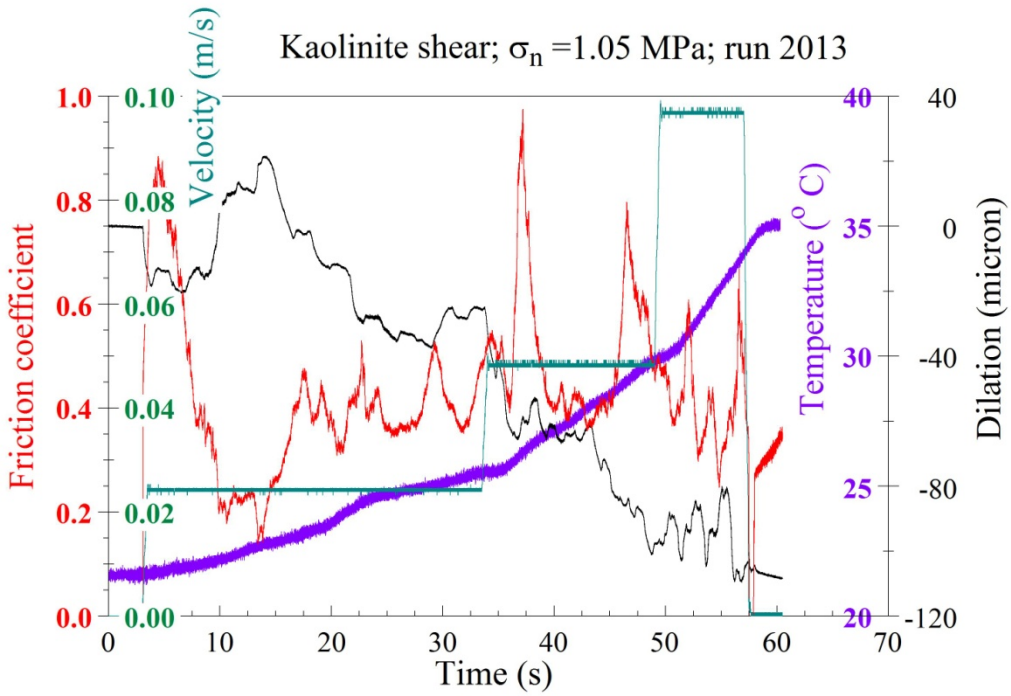

Fig. 12. Parametric observations during experiment 2013.

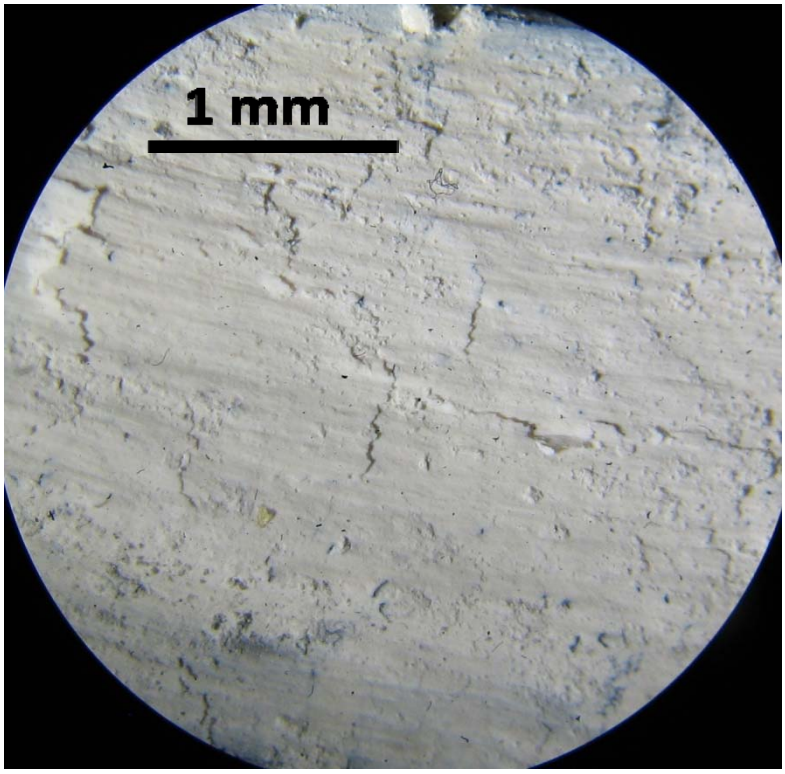

Fig.13. Left-View of a thin kaolinite cover that adhered to the glued sand on top of the loading hollow cylinder after an experiment. Note the slickenside striation within the kaolinite and the black dots of the quartz sand. . Right- close-up view revealing a few sand grains, ~ 200 mm in size, below the kaolinite adhered layer.

Fig. 14. A slickensided slip surface of a Riedel shear within the kaolinite layer.

Power control

Our new operation software is capable to run experiments under power control mode (details above). An example of such run on a steel-brass sample is shown in Fig. 15. Note the good agreement between the requested power density (red) and the measured power density (black).

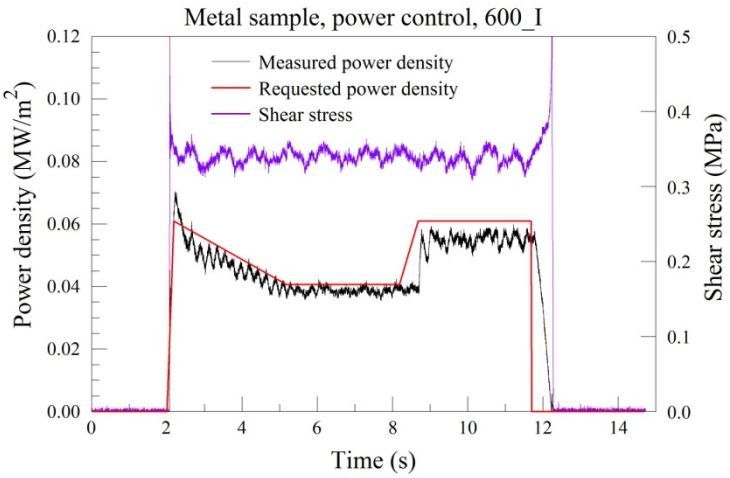

Fig. 15. Time plot of power controlled experiment on a steel-brass solid sample.

PLANNED EXPERIMENTS

Confined gouge experiments

We will start with monomineralic powders composed of quartz, kaolinite, calcite, k-feldspar and montmorillonite. We will continue with mixtures of these powders and fault gouge from three sources: clay powder from SAFOD, San Andreas gouge collected in Southern California, and rock powder formed during earthquakes in deep mines. Experimental procedures will include:

1. **Steady-state experiments**. Long slip (up to tens of meters) under constant velocity and constant normal stress. These experiments will provide the steady-state friction, heating, wear rate, volumetric changes in the gouge, and the dependence of all these parameters on the normal stress.
2. **Multiple stepping velocity**. We will run tests with stepping velocity from slow to high speed and vice versa (Figs. 11, 12). These experiments will show friction evolution under changing velocity, the effect of temperature (Fig. 13), and data on "short-term friction" values.
3. **Slide-hold-slide** e.g., Fig. 11. Tests will be run with hold times up to 10^5 sec. Previous studies showed that during hold periods, the fine-grain gouge may strengthen very fast and regain its strength within 24 hr.
4. **Pore-pressure experiments.** We will use the pore-pressure capabilities of CROC (above) to explore its effects on powder behavior and to measure the gouge permeability.

Analysis

The analysis will include these parts:

1. **Synthesis of the laboratory results** of the relationships between the various experimental parameters. The friction relation with velocity, hold time, slip history and temperature will be explored in details. This work will be done in our lab using standard and dedicated software.
2. **Characterization of gouge powder** at microscopic (thin-sections) and sub-microscopic (SEM, TEM and AFM) scales. Some of the analyses will be conducted before the friction tests and some after the tests. This work will be done in the University of Oklahoma and USGS Menlo Park (support letter).

E. REFERENCES

Brodsky, EE; Kanamori, H, 2001. Elastohydrodynamic lubrication of faults. JGR, 106, pp.16,357-16,374.

Chester FM, Chester JS, 1998, Ultracataclasite structure and friction processes of the Punchbowl fault, San Andreas system, California. Tectonophysics 295, 199-221.

Chester FM, Evans JP, Biegel RL, 1993. Internal structure and weakening mechanisms of the San-Andreas Fault. JGR, 98, 771-786.

Di Toro G, Goldsby DL, Tullis TE, 2004. Friction falls towards zero in quartz rock as slip velocity approaches seismic rates. Nature, 427, 436-439.

Heshmat H, 1995. The Quasi-Hydrodynamic Mechanism of Powder Lubrication—Part III: On Theory and Rheology of Triboparticulates. J Tribology Transactions, 38, pp 269 - 276

Higgs, CF, Heshmat CA, Heshmat H, 1999. Comparative evaluation of MoS_2 and WS_2 as powder lubricants in high speed, multi-pad journal bearings. J Tribology, ASME, 121 / 625-630

Jaeger, HM, Nagel, SR, Behringer, RP, 1996. Granular solids, liquids, and gases. Rev. Mod. Phys. 68, 1259–1273.

Kaur RG, Heshmat H, 2002. 100 mm Diameter Self-Contained Solid/Powder Lubricated Auxiliary Bearing Operated at 30,000 rpm," Lubr. Eng., 58, pp. 13–20.

Klausner JF, Dongming C., Renwei M., 2000.Experimental investigation of cohesive powder rheology. Powder Technology 112, 94–101

Latzel M, S. Luding, H.J. Herrmann, D.W. Howell, and R.P. Behringer, 2003. Comparing simulation and experiment of a 2D granular Couette shear device. Eur. Phys. J. E 11, 325–333

Lockner, DA; Naka, H; Tanaka, H; Ito, H; Ikeda, R, 2000. Permeability and strength of core samples for the Nojima Fault of the 1995 Kobe earthquake. USGS, OF 00-0129, pp.147-152.

Mair K, Marone C, 1999. Friction of simulated fault gouge for a wide range of velocities and normal stresses. JGR, 104, 28899-28914.

Marone C., 2004. Earthquake science Faults greased at high speed. Nature 427, 405-406

Noda H, Shimamoto T, 2005. Thermal pressurization and slip-weakening distance of a fault: An example of the Hanaore fault, southwest Japan. Bull Seism. Soc. Am., 95, 1224-1233.

Scholz CH, 2002. The Mechanics of Earthquakes and Faulting, Cambridge U Press, London, 471 pp.

Sibson, RH, 2003. Thickness of the seismic slip zone. Bull. SSA, 93, pp.1169-1178.

Tsutsumi, A; Shimamoto, T., 1997. High-velocity frictional properties of gabbro. GRL, 24, pp.699-702.

Tullis T., 2007, Laboratory Rock Mechanics Results: Frictional Resistance at Seismic slip Rates. Lecture at 2005 SCEC/USGS Extreme Ground Motion Workshop.

Wilson B., T.A. Dewers, Z. Reches, and J. Brune, 2005, Texture and Energetics of Gouge Powder from Earthquake Rupture Zones. Nature, 434, 749-752.

Wornyoh EA, Jasti VK, Higgs CF, 2007. A review of dry particulate lubrication: powder and granular materials. J Tribology, ASME, 129, 438-449

Yund, RA; Blanpied, ML; Tullis, TE; Weeks, JD, 1990. Amorphous material in high strain experimental fault gouges. JGR, 95, pp.15,589-15,60